Astron. Astrophys. 332, 939–957 (1998)

ASTRONOMY AND ASTROPHYSICS

Whole Earth Telescope observations of AM Canum Venaticorum – discoseismology at last

J.-E. Solheim[1,14], J.L. Provencal[2,15], P.A. Bradley[2,16], G. Vauclair[3], M.A. Barstow[4], S.O. Kepler[5], G. Fontaine[6], A.D. Grauer[7], D.E. Winget[2], T.M.K. Marar[8], E.M. Leibowitz[9], P.-I. Emanuelsen[1], M. Chevreton[10], N. Dolez[3], A. Kanaan[5], P. Bergeron[6], C.F. Claver[2,17], J.C. Clemens[2,18], S.J. Kleinman[2], B.P. Hine[12], S. Seetha[8], B.N. Ashoka[8], T. Mazeh[9], A.E. Sansom[4,19], R.W. Tweedy[4], E.G. Meištas[11,13], A. Bruvold[1], and C.M. Massacand[1]

[1] Nordlysobservatoriet, Institutt for Fysikk, Universitetet i Tromsø, N-9037 Tromsø, Norway
[2] McDonald Observatory and Department of Astronomy, The University of Texas at Austin, Austin, TX 78712, USA
[3] Observatoire Midi–Pyrenees, 14 Avenue E. Belin, F-31400 Toulouse, France
[4] Department of Physics and Astronomy, University of Leicester, Leicester, LE1 7RH, UK
[5] Instituto de Fisica, Universidade Federal do Rio Grande do Sul, 91500-970 Porto Alegre - RS, Brazil
[6] Department de Physique, Université de Montréal, C.P. 6128, Succ A., Montréal, PQ H3C 3J7, Canada
[7] Department of Physics and Astronomy, University of Arkansas, 2801 S. University Ave, Little Rock, AR 72204, USA
[8] Technical Physics Division, ISRO Satelite Centre, Airport Rd, Bangalore, 560 017 India
[9] University of Tel Aviv, Department of Physics and Astronomy, Ramat Aviv, Tel Aviv 69978, Israel
[10] Observatoire de Paris-Meudon, F-92195 Meudon Principal Cedex, France
[11] Institute of Material Research and Applied Sciences, Vilnius University, Ciurlionio 29, Vilnius 2009, Lithuania
[12] NASA Ames Research Center, M.S. 244-4, Moffett Field, CA 94035, USA
[13] Astronomical Observatory of the Institute of Theoretical Physics and Astronomy, Goštauto 12, Vilnius 2600, Lithuania
[14] University of Cape Town, Department of Astronomy (visiting), and McDonald Observatory and Department of Astronomy, The University of Texas at Austin, Texas, USA (visiting)
[15] Department of Physics, University of Delaware, Newark, DE 19716, USA
[16] XTA, MS B–220, Los Alamos National Laboratory, Los Alamos, NM 87545, USA
[17] Kitt Peak National Observatory, Tucson, AZ 85726, USA
[18] California Institute of Technology, 105-24, Pasadena, CA 91125, USA
[19] Center for Astrophysics, University of Central Lancashire, Preston, PR1 2HE, UK

Received 9 May 1997 / Accepted 11 December 1997

Abstract. We report the results of 143.2 hours of time-series photometry over a 12 day period for AM CVn (= HZ 29) as part of the Whole Earth Telescope (WET) project.[1] This star is believed to be an ultra-short period cataclysmic binary. In the temporal spectrum of the light curve we find a series of 5 harmonically related frequency mo dulations, some with sidebands with a constant frequency spacing of 20.8 μHz always on the high-frequency side. The set of harmonics has a fundamental frequency of 951 μHz. No modulation is detected at this frequency in the light curve. In addition, modulations with frequencies 972.5 and 988.9 μHz are detected with low amplitudes. The structure of the dominant 1903 μHz modulation explains part of the "phase jitter" observed earlier. The amplitude of this peak is modulated with a period of 13.32 ± 0.05 hrs. The same period is detected in absorption line shape modulations, most likely arising from variable aspects of the outer parts of the disk (Patterson et al. 1993).

The observed periodic light modulations can be explained as a combination of aspect variations of disk modifications due to tidally induced shocks as described by Savonie et al. (1994), which leads to a two-armed spiral structure, and the mode coupling model of Lubow (1991), which leads to a three-fold azimuthal symmetry in the outer parts of the disk and a prograde precessing wave. The two- and three-fold aszimuthal structures are stationary in the binary frame and explain the higher harmonics of the orbital period we observe in the light curve. This may be the first example of a successful disco- seismological interpretation.

In addition we propose that the variable amplitude modulation at 989 μHz may be explained as a g-mode pulsation, which indicates that the central white dwarf may be a DO with a hot envelope.

[1] Based on data obtained in observing time allocated by Mc Donald Observatory, Texas; Mauna Kea Observatory, Hawaii; Vainu Bappu Observatory, India; Wise Observa- tory, Israel; Haute-Provence Observatory, France; The Nordic Optical Telescope and the Isaac Newton Telescope at Roque de Los Muchachos Observatory, La Palma, Spain

Key words: stars: individual: AM Canum Venaticorum – novae, cataclysmic variables – stars: oscillations – white dwarfs – accretion, accretion disks

1. Introduction

AM CVn is the prototype of a small group of variable stars with remarkable properties. They are all very blue objects, showing only He I and, occasionally He II features, which can vary from absorption to emission, in their optical spectra. Their UV-spectra contain features from processed material as C, N, O and heavier elements (Solheim 1993a). Photometric variations with periods 15–45 minutes are interpreted as indicators of orbital periods far shorter than obtained for ordinary cataclysmic variables.

In addition to AM CVn, five other objects belong to this group: EC 15330–1403, CR Boo, V803 Cen, CP Eri and GP Com. They form a sequence with increasing photo- metric periods and changes in behaviour. The first part of the sequence includes AM CVn and EC 15330–1403, each with periods near 1000 s, constant mean magnitudes, and absorption spectra. The middle of the sequence is populated by CR Boo, V803 Cen and CP Eri, all of which undergo large amplitude outbursts upon which are superimposed periods ranging from 1600 to 1800 s, and whose spectra vary from absorption to emission. GP Com represents the end of the sequence, with the longest photometric period of 2800 s and an emission spectrum.

Only for GP Com is the orbital period spectroscopically detected. This sequence may indicate a dependence of mass transfer rate on orbital period. Smak (1983) calculated, for reasonable assumptions of mass ratios and orbital periods, that AM CVn has a high mass transfer rate and is in a perpetual high state, while GP Com has a low rate and is in a permanent low state. CR Boo, V803 Cen and CP Eri were found to have mass transfer rates which make them unstable to disk perturbations.

Our empirically derived dependence of mass transfer rate on orbital period implies that the AM CVn stars form an evolutionary sequence. The binary model for these objects, involving mass transfer from a low mass degenerate secondary to a more typical deg enerate white dwarf via an accretion disk, was first proposed by Faulkner et al. (1972). More recent calculations (Savonije et al. 1986) show that the donor secondary will be driven out of thermal equilibrium, whereby the star does not become fully deg enerate, but remains semi-degenerate. Warner (1995a) finds that a semi-degenerate secondary model gives reasonable primary masses for all the AM CVn objects.

The evolution of a pair of interacting degenerate stars with low mass ratio can produce white dwarf stars of different composition and masses than is possible with single star evolution. Nather et al. (1981) proposed that interacting binaries could evolve into single helium white dwarfs (DBs), which are normal (C/O core) white dwarfs showing He lines. Binary evolution may also explain the He core white dwarfs. Low mass single stars evolve too slowly to form the lighter helium core white dwarf stars in a Hubble time (Iben & Webbink 1989). It is therefore difficult to explain white dwarfs with masses less than 0.55 $M_\odot$ without binary star evolution (Iben & Tutukov 1986). Evolutionary calculations for white dwarfs with various compositions and a non-degenerate helium or hydrogen secondary star (Iben & Tutukov 1991) show that after several thermonuclear runaway flashes, during which helium rich shells are emitted, the secondary has a mass below 0.2 $M_\odot$ and no more flashes are expected. Mass transfer will strip the donor until a degenerate core of less than 0.1 $M_\odot$ remains, which will continue to transfer mass at a mass transfer rate $\lesssim 10^{-9}$ $M_\odot$/yr. In contrast to the short rapid transfer phases, the final slow transfer can last a few times 10^8 years, when the orbital period is slowly increasing. The study of this process, where the internal layers of the donor star are exposed, can give important clues to its earlier history, and gives us means to test theories of stellar evolution (Nather 1985).

AM CVn's IUE and HST UV spectra reveal absorption features of Si III, Si IV, N IV, N V, C IV, O V and He II (Solheim & Kjeldseth–Moe 1983; Solheim et al. 1997). If these features originate from an accreting white dwarf, we require a temperature of 50, 000–150,000 K. The wide absorption profile of He II (λ1640 Å) is almost identical to a similar profile for the coldest DO star HZ 21, and may indicate a connection between the central star of the AM CVn system and the DOs (Solheim & Sion 1994).

Non-radial oscillations have been proposed as a possible explanation of AM CVn's photometric variations. A class of pulsating white dwarfs, the DOVs, do exist within the central white dwarf's temperature range. The identification of a pulsating white dwarf within a binary system would provide a unique opportunity to probe, using the techniques of astro- seismology (Nather et al. 1990), the interior of an accreting star. We may expect to observe changes in the pulsation spectrum as a function of the mass transfer rate and the changes in the temperature profile of the accretor's atmosphere (Nitta 1996). However, if AM CVn's central star is a DO pulsator, we may have serious problems in detecting its pulsations in the optical part of the spectrum where the flux from the disk will dominate.

Even if we detect only a few pulsations for AM CVn, it would be of great interest, and a challenge to theoreticians to model the pulsation spectrum of pulsating accretors in the AM CVn systems. These objects may be examples of white dwarfs which are dist urbed from the outside by accreting matter dumped on them and triggering pulsations, which otherwise would not be observable. Parametric resonance with the secondary l ow mass object and possible pulsations in the disk may complicate the interpretation of the modulations we observe.

AM CVn has not changed its mean magnitude significantly in the more than 30 years it has been observed[2] (Sect. 2). A study of its properties may be justified by the possibility of identifying the orbital period and its harmonics which probe the disk, and the period of rotation of the central star, which may tell us if

[2] AM CVn was included in the Carlsberg Meridian Circle programme at La Palma in 1992 and 1993. The first year it was constant, while it in 1993 varied between V = 14.15 and 13.7 (Solheim 1995)

Table 1. Participating sites.

Observatory	Location	Longitude	Latitude	Telescopes (m)
Roque de los Muchachos	La Palma, Canary Islands	$-17^\circ 53'$	$28^\circ 46'$	$2.5, 2.6^{a)}$
McDonald	Mt. Locke, Texas	−104 01	30 40	2.1, 0.9, 0.8
U. of Hawaii	Mauna Kea, Hawaii	−155 28	19 49	0.6, 3.6
Vainu Bappu	Kavalur, India	78 50	12 34	1.0, 2.3
Wise	Mt. Ramon, Israel	34 46	30 36	1.0
Haute − Provence	St. Michel, France	5 43	43 56	1.9

[a)] Both the Nordic Optical Telescope and the Isaac Newton Telescope allocated time for this project.

a hot boundary layer is needed or not. g-mode pulsations, if detected, will give clues to the understanding of the structure, composition, and evolution of the accreting star. By combining spectroscopic and astroseismological information, we would be able to set firm limits for theories of stellar evolution.

Patterson et al. (1993) reported periodic absorption line profile modulation for AM CVn with a period of 13.4 hrs which they interpreted as a period of disk precession. In Sects. 4 and 5 we will show that this period also exists in the photo- metric temporal spectrum, indicating a connection between the spectroscopic and photometric observations.

We will give a summary of earlier photometric observations of AM CVn in Sect. 2, then we will describe the Whole Earth Telescope (WET) observations and the data reduction procedure in Sect. 3. In Sect. 4 we present an analysis of the data, and som e special problems they gave us. In Sect. 5 we discuss one model which may explain the observations. Finally, in Sect. 6 we draw conclusions and point out the direction for further observations and theoretical work to understand this system.

2. Previous photometric observations and some interpretations

The helium white dwarf AM CVn was discovered to be a small amplitude, short period variable star by J. Smak in 1962 (Smak 1967). For a long time it had the record as the shortest period binary system, and has been intensively observed as a test of general relativity predictions of angular momentum loss. The light curve has been described as double humped, with a period of approximately 1051 s (951.5 μHz), as well as sometimes single humped, a change also observed in some CVs (Warner & Robinson 1972). Despite heroic observational efforts, there exists no consensus on the identity of orbital period is or its possible variation with time (Solheim et al. 1984, hereinafter SRNK; Patterson et al. 1992, hereinafter PSHR).

To identify the orbital period and address concerns about the phase stability of the photometric variations, SRNK analysed new and old observations spanning 1968 to 1982, finding possible periods in the range of 1051.04 to 1051.212 s (951.438–951.283 μHz). The authors point out that all periods could be related to 1051.044 s (951.435 μHz) if corrections for possible cycle count errors arising from lunar aliasing are included. Based on this idea, SRNK found a period change of $-3.2 \pm 0.6 \times 10^{-12}$ s s^{-1}, but with a considerable scatter, or "phase jitter" up to 0.2 P, of a nonperiodic nature, as if the period drifted for several months, and is then readjusted to the average. Later observations (Seetha et al. 1990; Emanuelsen 1990) confirmed this $\dot{P}$ for observations including the 1989 observing season, giving $\dot{P} = (-3.7 \pm 0.4) \times 10^{-12}$ s s^{-1}. PSHR found the scatter to be too large, and that their observations did not fit this ephemeris.

SRNK also included analysis of the densely observed 1978 data set (Patterson et al. 1979), for the first time calculating the Fourier transform (FT) of the light curve. The authors found no power at the expected period of 1051 s (951.4 μHz), but instead at 525.6 s and 1011.4 s (1902.6 and 988.7 μHz). They proposed that the changes in the light curve from double to single humped were due to beating between these two periods on a time scale of 3.7 hrs. Additional power was also found at 350.4 s (2854 μHz). SRNK suggested that the 525.6 s (1902.6 μHz) modulation might represent a physical period present in the system, and proposed it as the rotation period of the accretor, based on the negative $\dot{P}$, which they interpreted as sign of accretion-driven spin-up.

Evidence shows that power has been present at 525.6 s (1902.6 μHz) and 1011 s (988.7 μHz) in AM CVn's FT since it was discovered to be variable. Re-analysis of the earliest observations from 1962 (Kruzewski & Semeniak 1993), as well as high speed photometry from 1976, 1978, 1982, 1987, 1988, 1990, and 1992 (Provencal et al. 1995) find the dominant power always to be at 1902.5 μHz. The amplitude of this peak is stable within the observing error, as are peaks at integer multiples of 951.3 μHz which itself is never detected. A peak at 988.7 μHz (1011.4 s) is present in all data sets but show large amplitude variations on time scales from days to months, and sometimes from night to night (Emanuelsen 1990).

The alias problem, which occurs when periodic gaps are present in the data, for example, when one combines data from successive nights at the same observatory, are serious in AM CVn's case. Although few periods are present, the strong flickering and suspected frequency variations make a short light curve look almost aperiodic (Fig. 2). In the following sections we will report WET observations for this object, and investi-

Table 2. Journal of observations for WET run in 1990 of AM CVn

Location and telescope	Run	Date	Time of run start (UT)	Length of observations (hrs)	Observers*
McDonald 0.8 m	pab-0024	22 Mar	4:57:00	6.689	PAB
Kavalur 2.3 m	k90-0112	22 Mar	19:40:00	1.230	TMK,SS,BNA
Kavalur 2.3 m	k90-0113	22 Mar	22:26:00	0.600	TMK,SS,BNA
Mauna Kea 0.6 m	a210	23 Mar	7:28:00	7.802	AG
Kavalur 2.3 m	k90-0115	23 Mar	16:17:50	1.322	TMK,SS,BNA
Kavalur 2.3 m	k90-0116	23 Mar	18:44:10	0.812	TMK,SS,BNA
Wise Obs 1 m	ren-0071	23 Mar	21:49:00	4.856	REN,EML
Kavalur 2.3 m	k90-0117	24 Mar	16:21:00	1.936	TMK,SS,BNA
Wise Obs 1 m	ren-0072	24 Mar	17:53:30	8.789	REN,EML
Kavalur 2.3 m	k90-0118	24 Mar	18:27:10	2.844	TMK,SS,BNA
Kavalur 2.3 m	k90-0120	24 Mar	22:22:11	0.986	TMK,SS,BNA
Mauna Kea 0.6 m	a212	25 Mar	11:39:00	3.378	AG
Wise Obs 1 m	ren-0073	25 Mar	17:38:00	9.011	REN,EML
McDonald 2.1 m	pab-0029	26 Mar	5:13:30	6.283	PAB
Kavalur 1 m	k40-0124	26 Mar	14:48:00	2.714	TMK,SS,BNA
Wise Obs 1 m	ren-0074	26 Mar	17:23:30	9.178	REN,EML
Mauna Kea 0.6 m	a213	27 Mar	6:30:00	8.872	AG
Wise Obs 1 m	ren-0075	27 Mar	17:16:10	9.050	REN,EML
Mauna Kea 0.6 m	a215	28 Mar	12:40:00	2.447	AG
Wise Obs. 1 m	ren-0077	29 Mar	0:12:10	2.133	REN,EML
McDonald 0.9 m	EN-0001	29 Mar	6:01:08	1.597	MF
McDonald 0.9 m	EN-0002	29 Mar	8:06:44	2.642	MF
Mauna Kea 1 m	a217	29 Mar	12:56:00	2.228	AG
Haute Prov 1.9 m	GV-0071	30 Mar	1:46:57	2.050	GV
Mauna Kea 0.6 m	a220	30 Mar	12:56:00	2.086	AG
Haute Prov 1.9 m	GV-0075	31 Mar	1:39:40	2.117	GV
McDonald 0.8 m	EN-0003	31 Mar	2:29:33	6.602	MF
Mauna Kea 0.6 m	CFC-0020	31 Mar	7:22:20	6.072	CFC
Mauna Kea 3.6 m	FBV-002	31 Mar	13:07:57	2.044	GF,PB
Haute Prov 1.9 m	GV-0079	1 Apr	1:50:30	1.936	GV
Mauna Kea 0.6 m	CFC-0023	1 Apr	6:09:10	9.053	CFC
Mauna Kea 0.6 m	CFC-0024	2 Apr	5:35:30	9.548	CFC
Mauna Kea 0.6 m	CFC-0025	3 Apr	5:50:20	4.253	CFC
				total 143.160 hrs	

*Observers : PAB : P.A. Bradley; AG : A. Grauer; GV : G. Vauclair; TMK : T.M.K. Marar; REN : R.E. Nather; CFC : C.F. Claver; SS : S. Seetha; EML : E.M. Leibowitz; GF : G. Fontaine; BNA : B.N. Ashoka; MF : Marion Frueh; PB : P. Brassard

gate which of the earlier observed periods were present, at least during the period of our observations.

3. WET observations and data reductions

AM CVn was one of the two main targets in a WET run organized in March/April 1990. WET (the Whole Earth Telescope) (Nather et al. 1990) is an international organization of observers who participate in coordinated campaigns in order to eliminate periodic gaps in the observing coverage. Such gaps introduce aliases into the Fourier transforms (FT's), greatly complicating the analysis of multiperiodic pulsators. Because of the object's northern declination, only observatories in the northern hemisphere, listed in Table 1, participated in this run.

All telescopes were equipped with two-star photometers, except at the CFHT and Haute-Provence observatories where three star photometers were used. Integration times were 10 s for all the individual runs listed in Table 2, comprising a total of 143.2 hrs spanning 12 days. All our photometers use blue-sensitive bi-alkali phototubes without filters to maximize signal-to-noise ratio. The response of the system is in the wavelength range λ3200–6000 Å (Kaly tis et al. 1997). The details of our data reduction procedure are presented in Nather et al. (1990), we summarise it here:

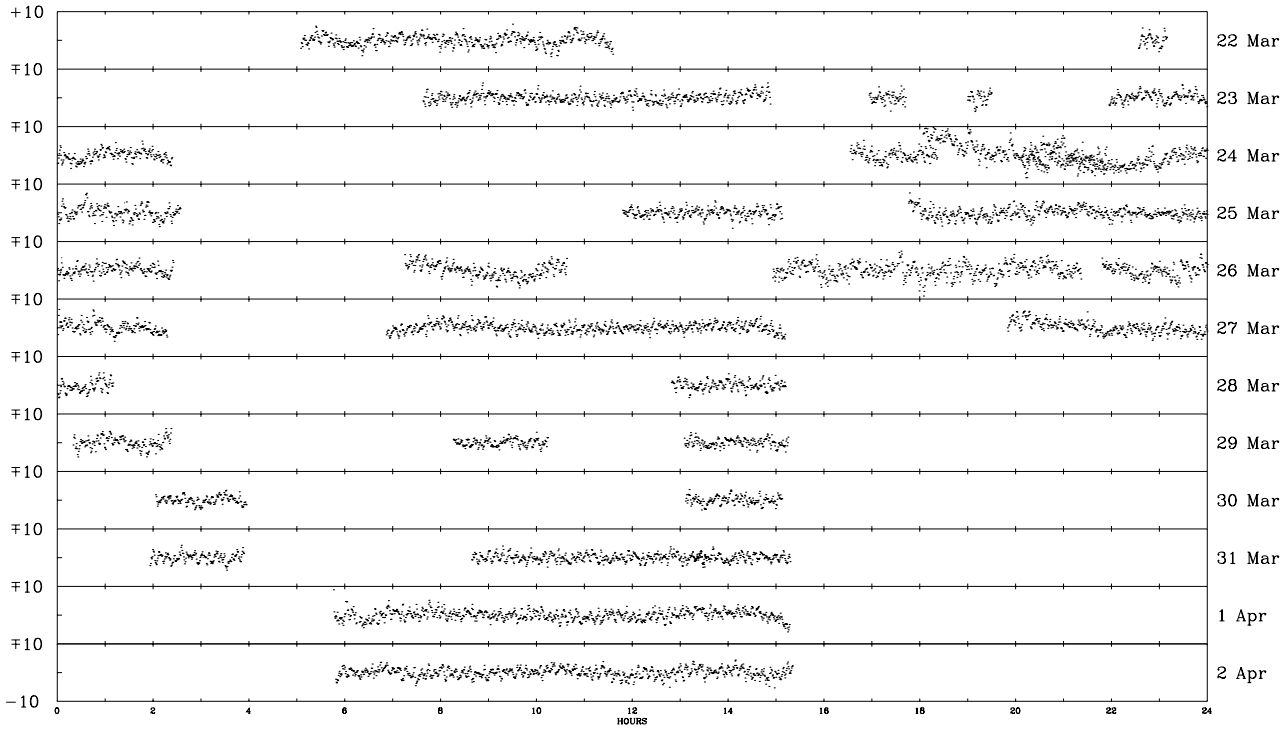

Fig. 1. The normalized light curve for the entire WET run. Each panel shows one day of data. The tickmarks on the ordinate scale represents 10 mmi. Each panel represents the light curve for one day. Time is in hours from midnight of the BJD of each day of the run

Both three-star photometers continuously monitored the sky background. For these data, we subtracted the sky point by point after cross-calibration and smoothing. Observers with two-channel photometers interrupted the observations of the target and comparison star for about 1 minute sky observations at irregular intervals – approximately every hour. We interpolated linearly between sky observations and subtracted the result from the data. The effects of extinction and other slow transparency variations were accounted for by fitting a third-order polynomial to each sky-subtracted data set and then dividing by this fit for normalising the data. We then subtracted the number one to obtain a mean of zero for all the data sets, producing light curves which show modulations in intensity (mi)[3] as a fraction of the total intensity, allowing us to combine light curves from different telescopes without further processing. The reduced WET light curve is shown in Fig. 1, where each panel spans 24 hours.

4. Data analysis

Since we had access to telescopes with sizes from 0.6 to 3.6 m, the S/N of the data varied. In Fig. 2 we show pieces of the light curve observed with the 3.6 and the 0.6 m telescopes at Mauna Kea on successive nights in the same hour angle interval. In the upper panel the light curve from the 3.6 m telescope is essentially noise-free, but the curve is still irregular. The next panel shows the light curve observed with the 0.6 m telescope, and it does not look significantly different. In the 3rd panel we show for comparison the light curve of PG 1159–035, a rich DO-pulsator of the same magnitude as AM CVn, observed with a 0.75 m telescope (Winget et al. 1991). In this case the pulses have small amplitudes but even with a small telescope a regular pattern is seen in the light curve.

A comparison of these light curves tells us immediately that AM CVn cannot be interpreted as a system with regular, small amplitude linear pulsations which is observed for some *g*-mode pulsating white dwarfs. We may have nonlinear pulsations or a combination of pulsations and flickering due to mass transfer.

Fig. 3 presents the Fourier Transform (FT) of the entire WET-run. Note the change in y-scale to accommodate the dynamic range of each panel. We find a series of peaks at 1902, 2853, 3805, 4756 and 5708 μHz. These peaks are numerically related to a fundamental frequency f_0 = 951 μHz – which itself is not detected. The 989 μHz peak which was present with large amplitudes in 1978, 1982 and 1987 (Provencal et al. 1995), has an amplitude of only 1.2 mma in this data set. Next we will describe the FT in general terms, then in the following subsections discuss details.

4.1. Results of the Fourier Transform in general terms

When we interpret the FT of a light curve we must be aware of its limitations when used on data sets with gaps. If we assume that some real modulation frequencies are present, the resolution and alias pattern generated by each real peak in the FT is described

[3] The unit mi refers to the fractional intensity (on a linear scale) relative to the mean brightness of the star. 100 per cent modulation is by definition 1 mi = 1000 mmi

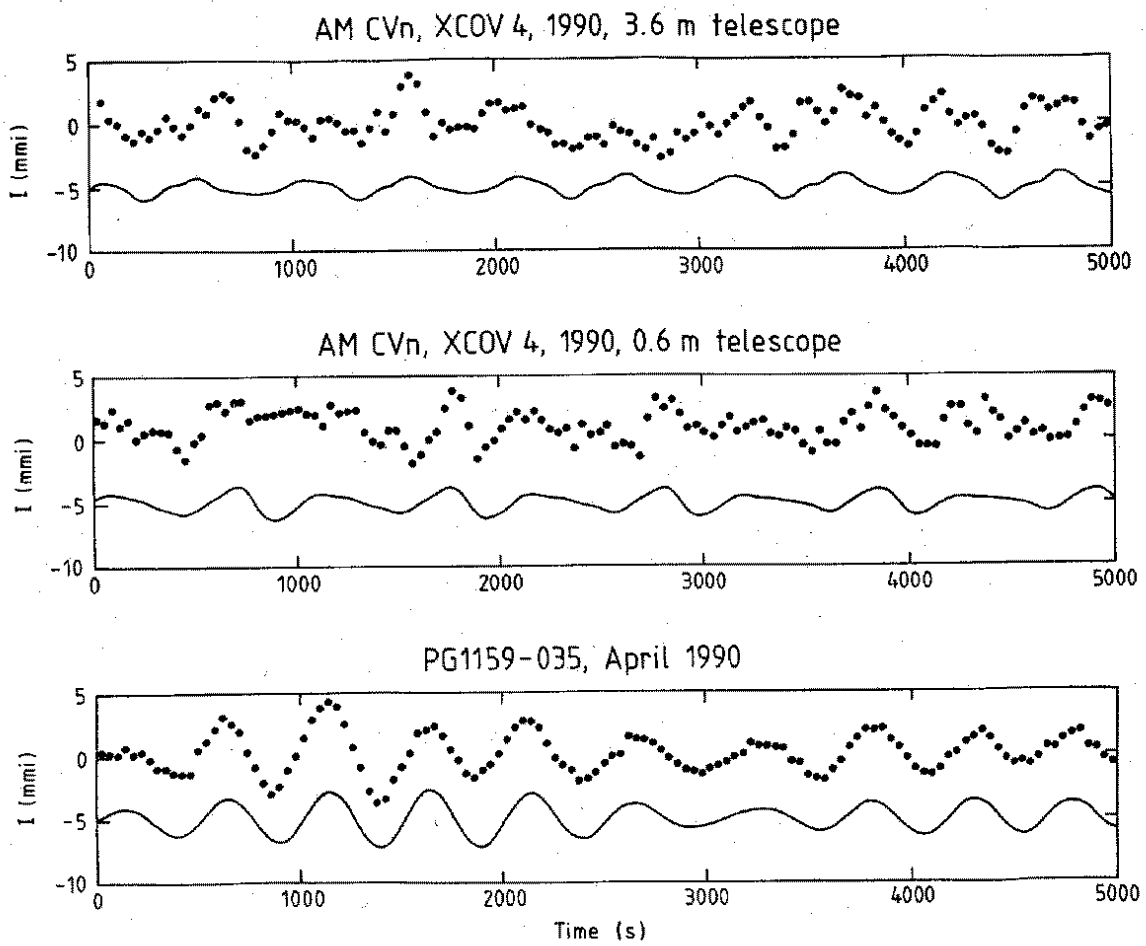

Fig. 2. Part of the light curve of AM CVn observed with the CFHT 3.6 m telescope is shown in the upper panel. The second panel shows the light curve 24 hrs later at the same location (Hawaii) observed with a 0.6 m telescope. The lower panel shows the light curve of a rich low amplitude pulsator PG 1159–035 observed with a 0.75 m telescope. The lower (solid) curve in each panel is a synthetic light curve calculated from the frequencies, amplitudes and phases determined. The unit mmi is milli-modulation intensity

by the spectral window, the pattern of peaks generated in a FT by a single sinusoid sampled exactly as the data (Nather et al. 1990). Our WET coverage was not complete, resulting in a spectral window containing small sidebands due to remaining periodic gaps in our data samples (Fig. 4). The temporal resolution of our FT, given as the inverse of the length of the campaign, is $1 \approx \mu$Hz.

The power spectrum's noise level begins to rise exponentially below 400 μHz, masking any real power in this part of the spectrum. Polynomial division forces the noise level to zero below 50 μHz, reducing our sensitivity to low frequency variations. The dominant peak is at 1903 μHz (= $2f_0$). We find additional peaks at each f_0 higher frequency up to 5708 μHz. In addition to this series of harmonics, there are other smaller peaks, but no obvious pattern is found.

We tested the stability of the resolved power spectrum with a simple comparison between the first and the second half of the run (Fig. 5). We find that the main peaks are present in both parts, but the higher harmonics are somewhat stronger in the second part. However, the lower priority and less favourable sampling in the second part of the run degrades our window function, reintroducing alias features and increasing the noise level, possibly accounting for the increased amplitude of the higher harmonics.

The most surprising and unexpected feature in the temporal spectrum is a sideband splitting of 20.8 μHz (or a period of 13.4 hrs) associated with some of the harmonics, always on the high frequency side.

4.2. Peaks in the 1000 μHz region

The question confronting us with AM CVn is the existence of a 951 μHz (1051 s) modulation. To settle this question we show an enlargement of the 1000 μHz region in Fig. 6. The only significant peaks in this region are at 972.3 μHz (1028.5 s), 988.8 (1011.4 s) and 1045 μHz (957 s), all with an amplitude about 1.2 mma. We have not seen the 1045 μHz power before, and the power previously reported at 976 μHz (Solheim et al. 1984) is not detected here. Most importantly, we conclude that the 951 μHz modulation is not detected in this data set.

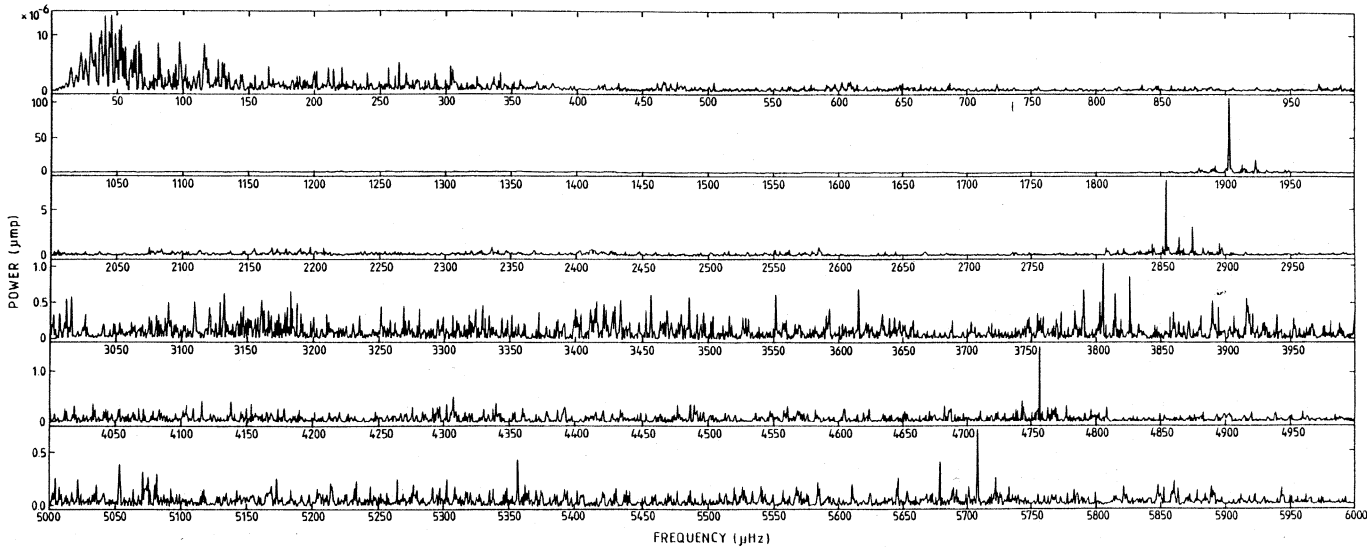

Fig. 3. Fourier Transform of the total data set. The ordinate shows relative power in units of μmp (modulation power which is $(\mathrm{ma})^2$). The ordinate scales are different for each panel in order to accommodate the range observed in each frequency interval. The frequency is in μHz

It is interesting to note that the 972.3 μHz peak is 21 μHz from the undetected f_0 at 951.3 μHz, the same sideband splitting as we find in the harmonics. We can therefore interpret it as a high frequency sideband to f_0. The 989 μHz peak has been observed at much larger amplitudes in the past, and is incommensurable with the set of numerically related frequencies. This modulation must have a different physical origin than the set of numerically related peaks. The 1045 μHz modulation has not been detected before and may either be spurious or a sideband to the 989 μHz peak, with a Δf = 56 μHz.

4.3. A search for constant frequency- and period splittings

Constant frequency and period spacings are frequently observed in the power spectra of classical hydrogen dwarf novae. Such frequencies could arise from beating with the orbital period or rotational period, g-mode pulsations or other causes. In a system with a disk we may not be able to observe the fine structure of the pulsation spectrum of the central white dwarf, but instead detect a pattern related to disk phenomena. To investigate this possibility we have searched the power spectrum for incidences of equal splittings with a method developed and described by Provencal (1994). This method does not require prior choices as inputs as in the KS (Kolmogorov–Smirnov) test. The method uses the spectral window to create a template containing two peaks separated by the frequency splitting of interest. This template is formed by adding, in both frequency and phase space, two spectral windows, one of which is offset by the frequency difference of interest with respect to the other. The template is then passed through the FT of the data set, and compared with the pattern of power surrounding every peak above an amplitude threshold decided upon by the user. The square of the difference between the template and the region around the actual peak is calculated, and summed for every peak above the amplitude limit. After each peak has been tested, a new template is created with a slightly different frequency splitting, and the process is repeated. The final product is an average difference for the entire FT, as function of the frequency splitting. If a certain splitting occurs in the FT a multiple of times, this will show up as a lower than average difference.

The result of the Provencal method used on the AM CVn data set is shown in Fig. 7. The two deep minima are aliases due to the data sampling, while the minimum at 21 μHz is the fine structure sidebands we have discovered. No additional splittings are detected.

4.4. Periods and phases of significant peaks

To verify the amplitude and phase of the sidebands of the harmonically related peaks, we prewhitened the data set in the following way: We identified the largest amplitude peak in a band, and subtracted a sinusoid with the same amplitude and phase from the light curve, repeating the process until no obvious peaks remained in the FT. An example of the prewhitening process for the 1902.5 μHz band is shown in Fig. 8. The exact periods, amplitudes and phases for the largest peaks were determined by a non-linear least square fit (Kepler 1993). The result is given in Table 3. Although f_0 = 951.3 μHz is itself undetected, we have adopted a naming strategy based on its numerical relationship to the other peaks. We have named the sequence of harmonics of the fundamental 951.3 μHz frequency for $h_1, ..., h_n$, where n identifies the nth harmonic. For the high frequency sidebands we add a second index 0, 1, or 2 to identify the sideband number. We have chosen 951.3 μHz as a fundamental frequency, since most of the observed frequencies fall into a harmonic pattern of this frequency. This is different from the conclusions of Provencal et al. (1995) who designate $2f_0$ (1902.5 μHz) as the fundamental frequency. As a time reference we have used the start of the WET campaign:

Table 3. Peaks detected or identified in the FT

Name	Freq. (μHz)	Period (s)	Amp (mma)†	Phase (s)	Noise (mma)†	Coherency
h_{01}	972.3	1028.48 ± 0.14	1.2	875 ± 78	0.4	Yes
$--$	988.8	1011.37 ± 0.09	1.2	709 ± 25		No?
h_{10}	1902.52	525.618 ± 0.003	10.4	27.4 ± 3.7		Yes
h_{11}	1923.36	519.923 ± 0.008	4.4	181 ± 9	0.4	Yes
h_{12}	1944.4	514.30 ± 0.03	1.2	81 ± 36		No
h_{20}	2853.82	350.407 ± 0.006	2.9	95 ± 9		Yes
h_{21}	2874.52	347.884 ± 0.009	1.8	185 ± 15	0.35	Yes
h_{22}	2895.4	345.379 ± 0.014	1.2	184 ± 23		No
h_{30}	3805.2	262.799 ± 0.009	1.0	202 ± 21		No
h_{31}	3825.9	261.379 ± 0.010	0.9	250 ± 23	0.3	Yes
h_{40}	4756.4	210.244 ± 0.005	1.25	168 ± 14	0.25	?(No)
h_{41}	4777.4	209.320 ± 0.010	0.6	21 ± 29		?(No)
h_{50}	5707.8	175.200 ± 0.005	0.9	172 ± 16	0.2	?(No)

†The unit ma is the modulation amplitude. 100 per cent modulation amplitude is by definition 1000 mma. The noise is defined as the average modulation in a frequency band excluding the peak and its window function

T_s = 2447972.711397 BJD. The phases given in the table refer to the first T_0 (for zero phase) after T_s.

We note that the "harmonic pattern" h_{10}, h_{20}, ..., h_{50} is very precise, with deviations from exact ratios of the order 10^{-5}. We have searched for, but not detected h_{60}.

The average sideband difference is 20.78 ± 0.12 μHz, corresponding to a period of 13.37 ± 0.07 hrs. Unfortunately, our observing and reduction technique, with subtraction of third order polynomials to remove long term variations, is not suited for detection of low frequency modulations in our temporal spectrum. However, we find that the amplitude of the strongest peak is modulated with this period, and will address this in Sect. 4.8 (Fig. 11).

We find no additional single peaks, except those given in Table 3. A band of excess power is seen between 1218 and 1248 μHz, and two peaks, each 1 mma are located at frequencies 1227 and 1307 μHz, but they seem to be unrelated to the set of harmonically related peaks in Table 3, and have a low signal to noise ratio. It should be noted that in an analysis of older data sets Provencal et al. (1995) have detected a power at $\frac{3}{2}h_{10}$ in some seasonal Fts.

The precise numerical relations between the frequencies $h_{10}, ..., h_{50}$ suggest that they are harmonics of one frequency ($f_0 = h_{10}/2$), and the constancy of the frequency splitting over a factor 3 in frequency range argues for a geometrical relationship which preserves the frequency splitting over such a range. In the following we will discuss the stability of the significant peaks, and how they modulate the light curve.

4.5. The stability of the significant peaks

To study the coherency of the various peaks we have divided the light curve in 9 parts, each of which are long enough to resolve the 21 μHz structure. We have fitted each subset, using linear least squares, with all of the frequencies determined above, to produce O–C diagrams to detect phase variations (Kepler 1993; Solheim 1993b).

To reduce the effect of aliasing, each part of the data set was prewhitened with the periods, amplitudes and phases given in Table 3, leaving only one peak in each group at a time for linear sinusoidal fit.

Examples of the resulting amplitude and phase variations after prewhitening are shown in Fig. 9. With some exceptions discussed below, the amplitudes and phases for the stronger peaks are constant. We can conclude that we have coherent oscillations in all of the harmonic peaks except h_{12}, h_{22} and h_{30}, which may have separate origins.

In the h_1 group (Fig. 8) the amplitudes are almost constant for h_{10} and h_{11}. The amplitude of h_{12} s is generally low (4 mma), but has a dramatic rise (to 14 mma) between day 6 and 9. This coincides with the rise in amplitude for h_{01}, indicating that these two periods are harmonically related, i.e. we may interpret h_{12} as a pulse shape harmonic of h_{01}. The phase of h_{10} shows no variations. The phase of h_{11} shows a systematic drift in the first part of the run, then jumps back to average around day 9. The phase of h_{12} jumps between two levels P/2 apart, again an indication that h_{12} is a pulse shape harmonic of h_{01}.

In the 350 s multiplet (h_{2i}) we also observe a constant amplitude except for an "event" taking place between day 6 and 9,

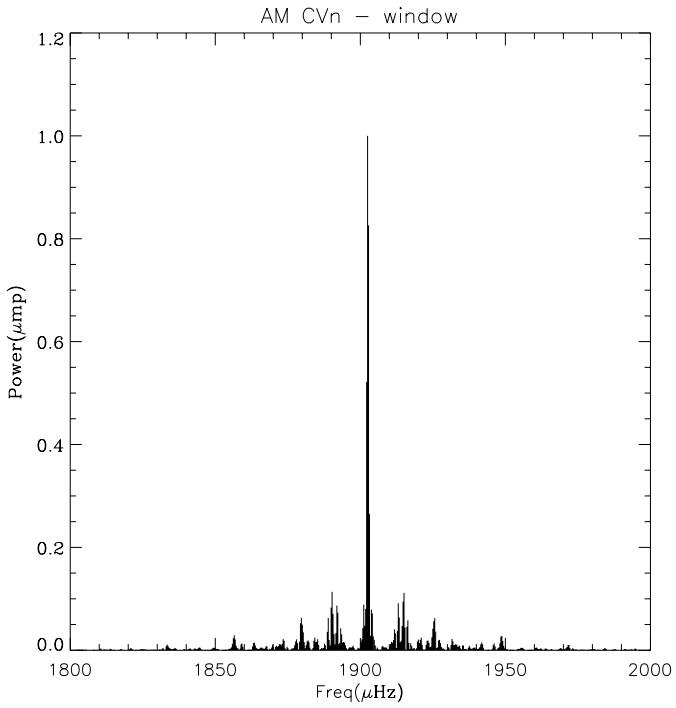

Fig. 4. The window function for the WET run on AM CVn. The sidebands are quite small and the resolution is about 1 μHz. The window function is in power and normalised to unity

which is strongest for h_{21}. The phase is drifting during the run for h_{21} and h_{22}.

In the remaining peaks (h_{30}–h_{50}) the event between day 6 and 9 is not observed. The amplitude of h_{30} is constant. The amplitude of h_{31} s slowly decreases during the run, while the amplitude of h_{40} slowly increases, making a sudden jump at the end of the run. The amplitude of h_{50} is only significantly different from zero in the central part of the run. We find no significant phase variations except a phase shift of P/2 at the very end of the run for h_{30}, indicating that this is a pulse shape harmonics of h_{10}.

We conclude that the peaks h_{10} and h_{20} are stable in amplitude and phase, while the peaks h_{01}, h_{11}, h_{21}, h_{22}, and h_{31} experience systematic drifts, and the rest are phase variable or uncertain in our data set. The periods h_{12} and h_{30} may be interpreted as pulse shape harmonics, while the others may represent real physical periods or beat periods. It should be emphasised that we can make only weak conclusions concerning the stability of the low amplitude modulations, and that we only discuss stability on time scales longer than 13.4 hrs. A summary of the stability of the strongest peaks is given in the last column of Table 3.

4.6. The average modulation shapes

We can find additional hints of the origin of AM CVn's photometric variations from a study of the average modulation shape. The average modulation shape is formed by folding a light curve at a period of interest. It contains the same information present in the FT, but provides an additional tool to interpret harmonic structures. We determined the average modulation shape of the dominant frequencies in AM CVn, and show some of them in Fig. 10.

The average modulation profile at the unseen fundamental frequency 951.3 μHz (Fig. 10a) shows one narrow and one wide peak per period. This difference has led previous observers (see Solheim et al. (1984) for a review) to identify these as primary and secondary maxima. If the two humps were equal, we would observe only the first harmonics in the FT. The higher harmonics will make two consecutive peaks of h_{10} look different. All the observed harmonically related frequencies could be interpreted as pulse shape harmonics of the fundamental frequency. However, since the harmonics are phase stable to the limit of detection (possibly except h_{30}), and have relatively constant amplitudes (Solheim 1993b), they can also be due to modulation of physical features. An argument against the sequence being simple harmonics of a fundamental frequency, is our expectation that the frequency splitting in that case would increase proportional to the order of the harmonics, while we observe a constant splitting.

The profile of h_{01} = 972.3 μHz (Fig. 10b) is almost sawtoothed and variable in shape, and requires higher order pulse shape harmonics to be explained. The lack of coherency for h_{12} and the amplitude correlation with h_{01} indicates that h_{12} (1944.4 μHz) is a pulse shape harmonics of h_{01}. If this frequency refers to a physical structure, it must have an irregular shape, and change on a short time scale. Higher order harmonics of the h_{01} pulse are not detected.

The sideband h_{11} and most of the remaining peaks investigated are all close to pure sinusoids. In Figs. 10c and 10d we show 988.8 μHz and h_{11} = 1923.4 μHz as examples. The coherency of the sidebands and their sinusoidal form indicate that they are aspect modulations. The 988.8 μHz modulation shows considerable seasonal variations (Provencal et al. 1995), arguing for the origin of this frequency in some feature which varies in size and shape. A lack of sidebands and the temporal instability for h_{50} argues for it being a pulse-shape harmonics for h_{20}. The same is the case for h_{30} which jumps $P/2$ in phase, as expected from pulse-shape harmonics.

4.7. A 13.32 hrs period detected

Patterson et al. (1993) report modulation of AM CVn's absorption line profiles with a period of 13.38 h, which they interpret as the precession period of an elliptical disk in the AM CVn system. The disk precession may be the cause of the 20.8 μHz frequency splitting we observe.

To investigate the effect of the precession period on the amplitude of h_{10}, we have fitted, using linear least squares, with a fixed period P = 525.62 s (1902.5 μHz) to sections of the data about 4 cycles ($\sim$ 35 minutes) in length, resulting in 176 amplitude determinations which we have folded with the period $P = 13^{\rm h}.4$ and shown in Fig. 11, This method is similar to the technique employed by Kurtz et al. (1989) for detection of precession in magnetic Ap stars.

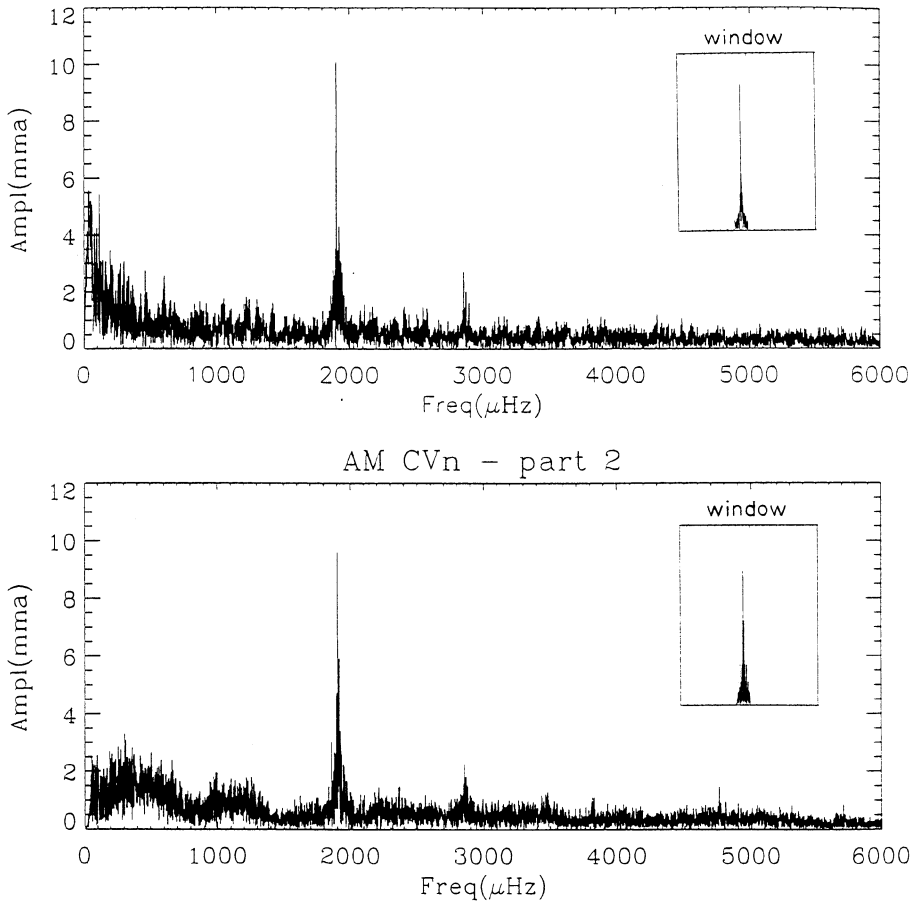

Fig. 5. Amplitude-FT of the first and second half of the run, with inserts showing the window functions in amplitude for each part

The large scatter in the diagram is due to the error in determination of amplitudes in the short light curve pieces. The upper envelope of the points shows the sinusoidal amplitude modulation expected from two unresolved nearby frequencies.

The period of the amplitude modulation and its time of maximum is determined by a non-linear least square analysis of the amplitude versus time distribution. We get as the period of amplitude modulation:

$P_{\rm am} = 13^{\rm h}.32 \pm 0.05$

or

$f_{\rm am} = 20.86 \pm 0.08\ \mu$Hz

and

$T_{\rm max} = 4^{\rm h}.4 \pm 0.6$ after T_0
$= 7972.895 \pm 0.025$ BJD

If we compare $T_{\rm max}$ with the phase of skewness variations determined by Patterson et al. (1993) for the broad absorption lines, we find their maximum value of skewness at T = 7972.867 BJD, which is in phase with our maximum amplitude. This strengthens the idea that the 1902.5 μHz modulation and the line skewness are related.

If we compare the various modulation periods, we find:

Period of amplitude modulation	$13^{\rm h}.32 \pm 0.05$
Period of multiplet splitting	$13^{\rm h}.37 \pm 0.07$ (Sect. 4.4)
Period of line skewness modulation	$13^{\rm h}.38 \pm 0.07$ (Patterson et al.)

We conclude that these periods are all the same within the error of measurement and are most likely related to the same phenomenon.

5. Discussion

The intense WET observing campaign representing almost half the existing photometry of this system has produced a unique data set on AM CVn.

Given all the spectroscopic and photometric evidence, we have great difficulty in interpreting AM CVn as a single star, although it has many properties in common with single white dwarfs (Patterson et al. 1992; Provencal et al. 1995).

A model for the system must explain the following observations:

- the numerical relationship between the h_{10}, h_{20}, ..., and h_{50} modulations
- the lack of power at f_0 = 951.3 μHz
- the 20.8 μHz sidebands associated with 4 of the harmonics ($h_1 ... h_4$)

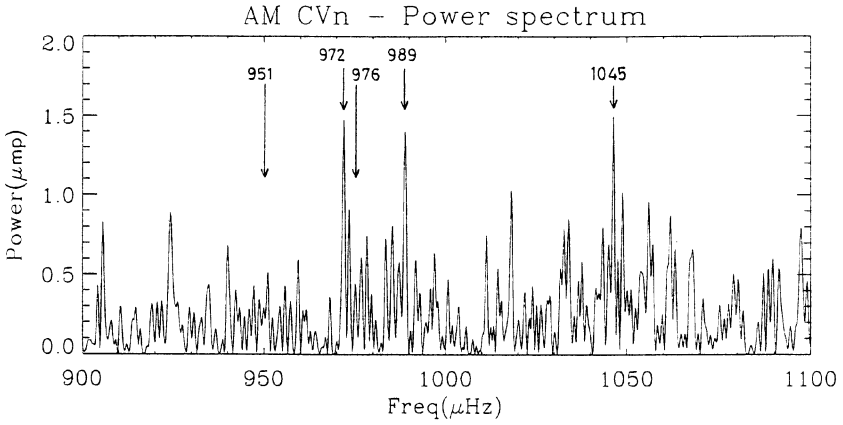

Fig. 6. Power spectrum of the region 900–1100 μHz with the frequencies corresponding to some of the interesting frequencies (951, 972, 976, and 1045 μHz) marked with arrows

– the amplitude modulation of the h_{10} = 1902.5 μHz peak in phase with the maximum absorption line skewness modulation observed by Patterson et al. (1993)
– the unrelated 988.8 μHz modulation
– the low amplitude peak at 972.3μHz which is f_0 + 21 μHz (h_{01})
– that the modulations at h_{12},h_{30} and maybe h_{50} are pulse shape harmonics
– the long time phase stability of the 1902.5μHz modulation with $\dot{P} = (1.71 \pm 0.04) \times 10^{-11}$ s s^{-1} (Provencal et al. 1995)

In addition, AM CVn's UV and optical spectra are complex, containing broad asymmetric features, P Cygni profiles of UV-resonance lines indicative of a wind, and a continuum spectrum which indicate a very hot central region, possibly containing a white dwarf (Solheim 1993c; Solheim & Sion 1994; Bard 1995).

5.1. The precessing disk model

Possible explanations for the system are discussed by Patterson et al. (1993) and Provencal et al. (1995). In the following we concentrate on one model which gives a simple explanation of nearly all the observations. It is a variation of the precessing disk model proposed for the AM CVn system by Patterson et al. (1993). They proposed that the 20.8 μHz modulation of the spectral lines is due to a prograde precessing apsidal line in an elliptical disk (Ω_b), and that f_0 = 951.3 μHz is the superhump frequency (Ω_s).

We will accept the explanation for the identification of Ω_b, but we find it more likely that f_0 is identified as the orbital frequency – because of the long term phase and amplitude stability of $h_{10} = 2f_0$, and because this peak always has most power.

Numerical simulations show that superhump periods exist in systems where the mass ratio is smaller than a critical ratio of q_c = 0.22 if the mass transfer rate is large enough (Whitehurst 1988; Osaki 1989; Lubow 1991). The key factor for development of an eccentric disk with observable superhumps is expansion of the disk beyond the critical radius for the 3:1 resonance between the orbital frequency and particle orbital frequencies. Ichikawa et al. (1993) show that such expansion can happen during a normal dwarf nova outburst. If the mass transfer rate is greater than $\dot{M}_{\rm crit}$, the system will go into a permanent super-outburst, and may show continuous super- humps (Osaki 1995, 1996). AM CVn's absorption line spectrum, flux distribution, and extreme mass ratio suggests a system in constant super-outburst, providing us with an excellent laboratory to study accretion and the superhump phenomenon. This has precedence: permanent superhumpers exist also among the hydrogen CVs. PG 0917 + 142 (Skillman & Patterson 1993) is a recent example, and we propose that the high mass transfer objects AM CVn and EC 15330–1403 are their helium CV counterparts. The absorption line profile modulation observed by Patterson et al. (1993) can be explained as due to the change of aspect angle with P_b, which also modulates the amplitude of the 1902.5 μHz frequency in the light curve.

It should be noted that the generally adopted interpretation of the superhump phenomenon in terms of a precessing disk based on numerical results by Whitehurst, Lubow and Ichikawa etc. is by no means well established. These results were obtained with quasi-particle codes (SPH or otherwise) with limited spatial resolution and high intrinsic viscosity. Calculations with *hydrodynamic* finite different codes yield different results. The dominant term in the tidal potential has m = 2, i.e. two-fold azimuthal structure. Indeed, the results of hydrodynamic calculations using the full tidal (point mass) potential of the secondary star show a strong two-armed spiral tidal (shock)wave in the disk, corotating with the companion. The dissipation in this shock wave detorques the disk material in the outer regions whereby the disk gets an elliptical shape which is fixed in the binary frame (e.g., see Fig. 10 in Savonije et al. (1994)). Recently, such an m = 2 tidal shock wave has in fact been observed in the CV IP Pegasi during outburst (Steeghs et al. 1997). In the SPH calculations no such clear m = 2 spiral structure is visible, instead the disk becomes eccentric and starts to precess. Precessing disks could only be obtained in the hydro calculations if (artificially) only the (weaker) m = 3 tidal component was applied and the precession disappeared once the full tide (including the dominant m = 2 component) was applied to the disk (Heemskerk 1994). Therefore the precessing disk model is at least open to debate. However, in the case of AM CVn we cannot have an elliptical shape which is fixed in the binary frame. This would give a f_0 modulation as soon as the inclination is > 0. However, observations of superhumps suggest

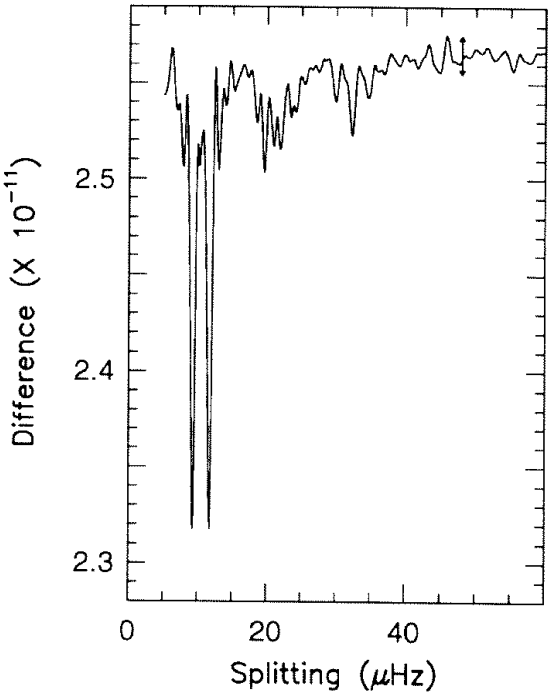

Fig. 7. Equal frequency splittings in the 1990 AM CVn FT. The deepest minima are window artefacts. The minima at 20.8 μHz is the fine structure associated with the 1902.5, 2853.8, and 3805 μHz frequencies (Provencal 1994). The bar at 47 μHz is a one sigma significance level

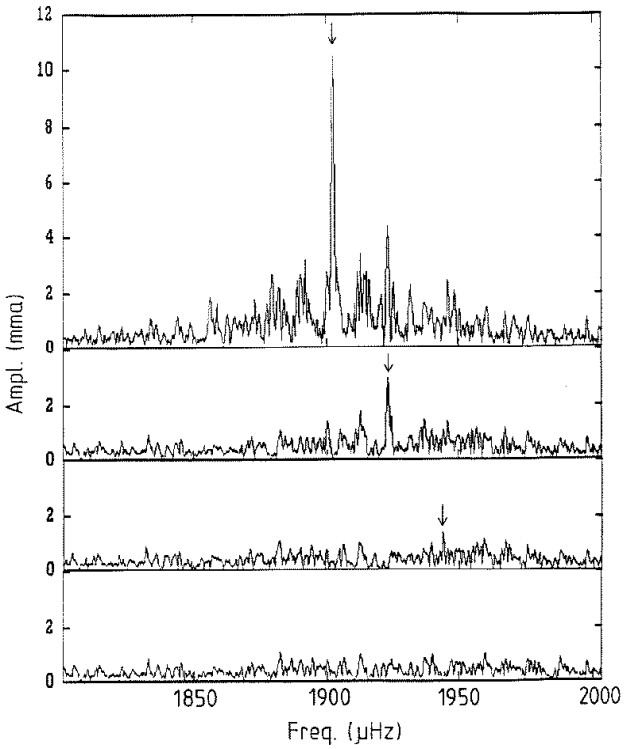

Fig. 8. The prewhitening process shown for the 1902.5 μHz region. The upper panels show the original FT, and the lower panels show the pattern left after successive subtraction of single sinusoids marked with arrows

indeed a slow precessional motion in the disk during its permanent superoutburst. If one accepts this model the following remarks are relevant:

If we in the binary frame have a prograde precessing disk, an observer in an inertial frame would observe as the superhump frequency:

$$\Omega_{\rm s} = \Omega_{\rm orb} + \Omega_{\rm b} \quad (1)$$

or

$$\frac{1}{P_{\rm s}} = \frac{1}{P_{\rm orb}} + \frac{1}{P_{\rm b}}$$

When we identify f_0 = 951.3 as $\Omega_{\rm orb}$, we get $\Omega_{\rm s}$ = 972.3 μHz or $P_{\rm s}$ = 1028.5 s, which we have detected as a low amplitude coherent modulation (Table 3). We find that $\Omega_{\rm b}$ is in good agreement with the disk apse precession rate $\Omega_{\rm b} = 0.022\,\Omega_{\rm orb}$ found by numerical simulations by Lubow (1991).

We observe beat between the binary orbital frequency and the prograde precession as $P_{\rm s} < P_{\rm orb}$. This is *not consistent* with the observed fact that all SU UMa stars show superhump periods $P_{\rm s}$ which are slightly longer than the orbital periods. Warner (1995b, Table 3.3) shows that for the SU UMa stars the superhump period is $\sim$ 3% longer than the orbital period. In order to observe the prograde precession as a shorter superhump period, we have to observe features in the disk in a fixed frame relative to the observer, and this will give us valuable information in modelling the disk shape. We conclude that the AM CVn system displays a mixture of properties from the two competing theories:

Since most power is seen in the peak at frequency 1902.5 μHz it must indeed correspond with the expected two-armed tidal spiral wave rotating with the orbital angular speed which, presumably due to aspect variation, gives a photometric signal modulated with twice the orbital frequency. Hence $\Omega_{\rm orb} \simeq 951$ μHz. The modulation at 3 times $\Omega_{\rm orb}$ can be interpreted as the weaker $m = 3$ tidal response of the disk which may arise when the disk has expanded in size. It may also be interpreted as a two-fold spiral rotating with 3/2 times $\Omega_{\rm orb}$, as expected from Lubow's non-linear wave interaction model. However, if the signal h_{40} (at $5\Omega_{\rm orb}$) is real, it is difficult to explain in Lubow's model. In his model h_{20} would correspond to a two-fold spiral moving with 1.5 times the orbital angular speed. In combination with the observed two-fold tidal spiral (h_{10}) this could never give rise to time variation with $5\Omega_{\rm orb}$. But in terms of direct tidal responses it could be the combined time-signal of a two-fold and a three-fold spiral wave both moving with the orbital angular speed through the disk.

The components with the above frequencies plus 20.8 μHz could then be interpreted in terms of their interaction with a precessing (with $\Omega_{\rm orb} + \epsilon$) eccentric $m = 1$ mode, whereby ϵ = 20.8 μHz. However, the peaks with the above-mentioned main frequencies plus *twice* 20.8 μHz remain unexplained.

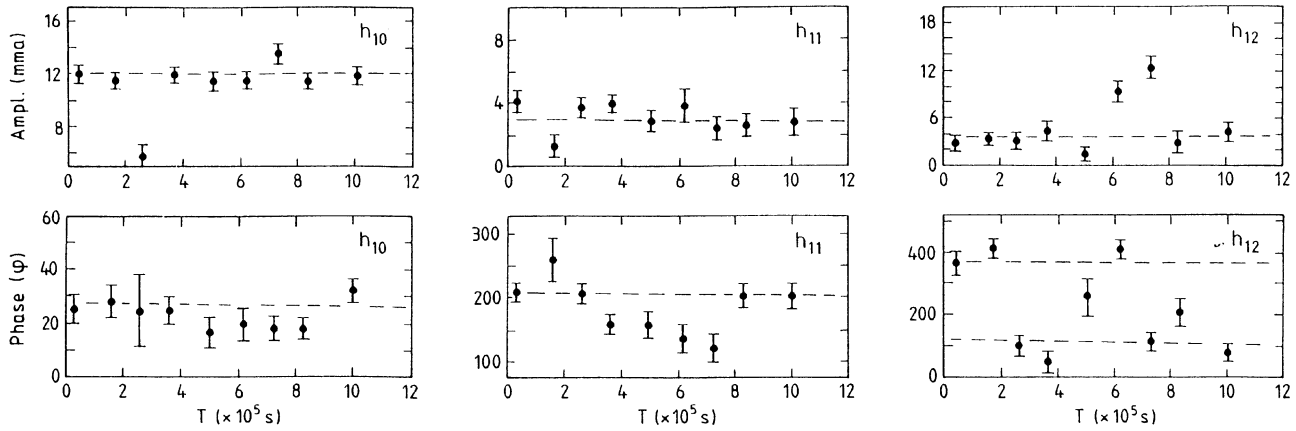

Fig. 9. Amplitude and phase variations for the strongest (h_1) group (1903 μHz) during the campaign. The top panels show amplitude variations and the lower panels show the phase variations. The abscissa unit is 10^5 s, and the ordinate unit of the upper panels is mma (milli-modulation amplitude), while the ordinate unit of the lower panels is s

However, h_{12} is probably a pulse-shape harmonic, while h_{22} may be spurious or $2\Omega_{\rm orb} + \Omega_{\rm s} + \Omega_{\rm b}$.

Simulations of disks in systems with small mass ratios demonstrate that the difference between $P_{\rm b}$ and $P_{\rm orb}$ diminishes with declining mass ratio (Hirose & Osaki 1990). A relation between $P_{\rm b}$ and $P_{\rm orb}$ has been established by Warner (1995b):

$$\frac{P_{\rm b}}{P_{\rm orb}} = A\,\frac{1+q}{q} \qquad (2)$$

where A = 3.73 for $0.05 < q < 0.1$. When we identify $P_{\rm b}$ = $13^{\rm h}.4$ and $P_{\rm orb}$ = 1051.2 s we get q = 0.088.

The secondaries in AM CVn systems have never been directly observed. Theoretical modelling has led to two possibilities concerning their nature. The first one assumes a completely degenerate secondary as proposed by Faulkner et al. (1972). Using q = 0.088, we find M_2 = 0.031 $M_\odot$ and M_1 = 0.35 $M_\odot$. The second possibility is to accept the conclusions of Savonije et al. (1986) who demonstrate that the high mass transfer rate drives the secondary out of thermal equilibrium and keeps it semi-degenerate. In this case the mass radius relation (Savonije et al. 1986) gives M_2 = 0.087 $M_\odot$ and M_1 = 0.99 $M_\odot$. The semi-degenerate solution gives a reasonable fit for all the AM CVn stars, while solutions for fully degenerate secondaries give too low mass for the primary in most cases (Warner 1995a). As radius of the accreting star we use the Hansen and Kawaler (1994) formula for a C–O white dwarf intermediate between non-relativistic and full-relativistic degeneracy, which gives r_* = 5600 km.

We can also use the assumption that AM CVn is in permanent superoutburst and compare $\dot{M}_{\rm crit}$ for the two choices of the stellar masses. We use the following equation from Smak (1983)

$$\dot{M}_{\rm crit} = \frac{8M}{3}\,\sigma T_{\rm eff}^4\,\frac{r_d}{1-\mu}\left(\frac{P_{\rm orb}}{2\pi}\right)^2\left[1-\left(\frac{r_*}{r_d}\right)^{1/2}\right]^{-1} \qquad (3)$$

where $\dot{M}_{\rm crit}$ is the minimum mass transfer rate for a constant high state, where $\mu = M_1/(M_1+M_2)$, r_d is the disk radius, and r_* is the radius of the accreting white dwarf. As disk radius we use $0.48a$, which is the tidal radius of the disk (Hirose & Osaki 1989). For M_1 = 0.38 $M_\odot$ we get $\dot{M}_{\rm crit}$ = 9×10^{16} g/s, and for M_1 = 1.0 $M_\odot$ we get $\dot{M}_{\rm crit}$ = 5×10^{16} g/s. The best fit to the observed continuum disk spectrum based on stellar atmosphere models, gives $\dot{M}$ = 6.4×10^{16} g/s (Bard 1995), which give us another argument for the high mass solution which we will adopt in the following.

If the maximum and minimum velocities determined from the absorption lines originate in the disk, we can determine limits for mass and inclination (Patterson et al. 1993; Warner 1995a). The only solution for M_1 = 1.0 $M_\odot$ is an inclination of $i \sim 40$ degrees, which requires an inner disk radius of 2.1 r_*.

With $P_{\rm orb}$ = 1051.2 s and $P_{\rm s}$ = 1028.5 s, we obtain a beat frequency of 21 μHz (Eq. (1)) which may be present as high frequency sidebands to all physical frequencies in the system. This gives us an added bonus – we can use the 21 μHz frequency splitting to identify disk related physical frequencies. We also expect to observe some sum and difference frequencies and pulse-shape harmonics as is commonly observed in systems with non-sinusoidal modulations.

For the modulation at the independent frequency of 988.8 μHz, we may challenge the origin proposed by Patterson et al. (1993). They suggest that the 988.8 μHz frequency is a beat frequency resulting from a 16.5 μHz (or period 16.8 hrs) retrograde precession of the line of nodes in a slightly tilted disk. This would result in low frequency sidebands or amplitude modulations with this frequency which we have searched for, but did not find in our data. This search may be more profitable when the amplitude of the 988.8 μHz modulation is high. From a study of absorption line variations Patterson et al. (1993) conclude that the tilt could be at most a few degrees.

Patterson et al.'s (1993) proposed identification of the 988.8 μHz modulation as a disk tilt frequency is based on their identification of 972.3 μHz as the orbital frequency. Our identification of 951.3 μHz as the orbital frequency and 972.3 μHz as the (prograde) superhump frequency, leads to a prediction of

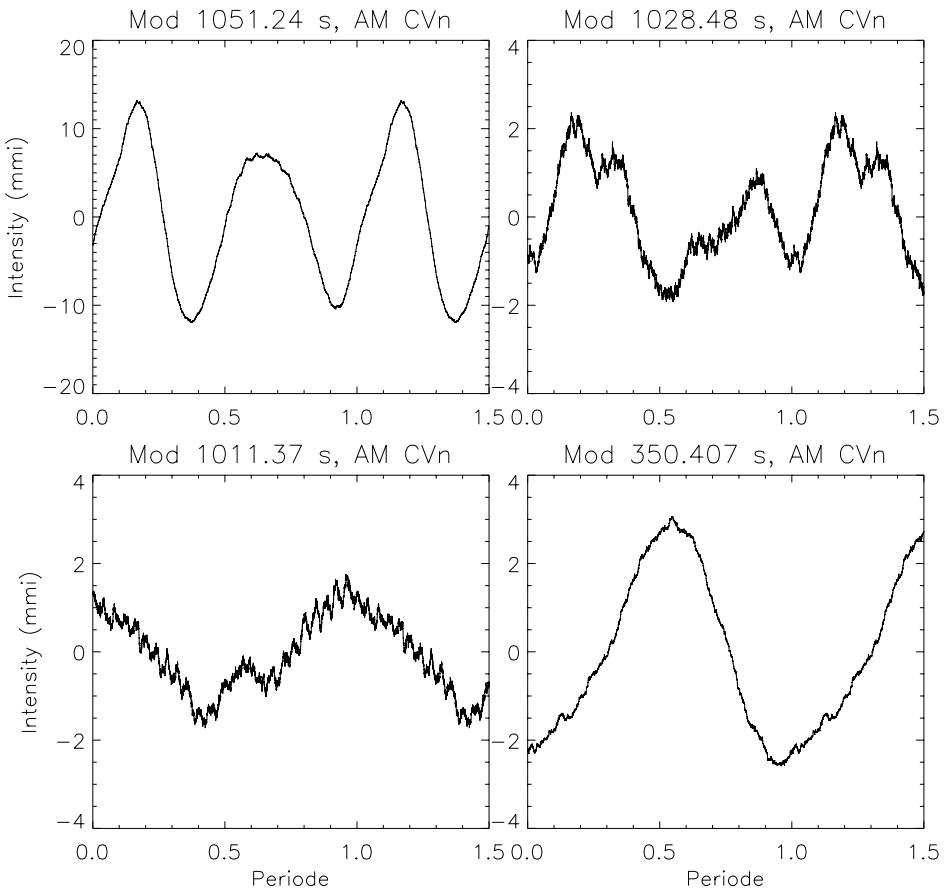

Fig. 10a–d. Pulse shape for 4 modulations. **a** h_{00} = 951.3 μHz, **b** h_{01} = 972.3 μHz, **c** 988.8 μHz, and **d** h_{20} = 2853.8 μHz. The ordinates are modulation intensity (mmi)

a lower frequency $\Omega_{\rm orb} - \Omega_{\rm n}$ for a beat between the (retrograde) nodal regression frequency ($\Omega_{\rm n}$) and the orbital frequency. Such a modulation is not detected, which may mean that a tilt is small or not present.

The amplitude variable modulation at 988.8 μHz is left unexplained by the expected disk frequencies. We have two possible other explanations for this modulation: It could either be the frequency of rotation $\Omega_{\rm rot}$ or a g-mode pulsation of the accreting white dwarf. If we observe $\Omega_{\rm rot}$ it must be due to the variable aspect of the accretion column on one of the poles. For both explanations we would expect higher amplitudes in the far UV, which is observed in HST spectra (Solheim et al. 1997). Arguments against the frequency of rotation interpretation are the rapid amplitude changes observed, no X-ray modulation at this frequency, and no polarization detected. AM CVn shows soft X-ray luminosities far below what is derived for polar systems, but not totally inconsistent with X-ray luminosities of non-magnetic CV's (Ulla 1995).

The implications of explaining the 988.8 μHz as a g-mode pulsation will be further discussed in Sect. 5.

5.2. The missing power at f_0 explained by a two-fold azimuthal structure or two spiral arms

We now consider a long standing problem for AM CVn: Why do we not observe any power at the fundamental orbital frequency $\Omega_{\rm orb}$, which we do for the other permanent superhumper in the AM CVn family, EC 15330–1403?

Any explanation of this problem would involve a phenomenon that happens twice per orbital period, and looks exactly the same each time. One possibility proposed by Solheim et al. (1984) and worked out in more detail by Provencal et al. (1995) is an intermediate polar system where a magnetic field sweeps a hole in the disk and the two accreting poles are seen twice per orbital revolution. In this case, we expect a negative $\dot{P}$ because the accretor will be spinning up (Solheim et al. 1984) or a positive $\dot{P}$ if the magnetic field is coupled to the slower rotating outer part of the disk (Provencal et al. 1995). An argument in favour of this model is that a hole in the disk is required to explain the maximum and minimum velocities in the disk with the high mass for the primary object, as described in the previous section.

We find several arguments against this interpretation. First, a magnetic field is not observed, although the small field required may escape detection. In addition, we do not find the variable X-ray emission expected from accreting columns (Ulla 1995). ROSAT observations of AM CVn can be interpreted as consisting of two sources: A blackbody source consistent with a white dwarf of $T_{\rm eff} < 86,000$ K, assuming $n_H = 10^{20}$, or $T_{\rm eff} \lesssim 157,000$ K, assuming $n_H = 10^{21}$, and an extra hard (bremsstrahlung) component with a temperature of a few keV, where n_H is the interstellar hydrogen column density in the di-

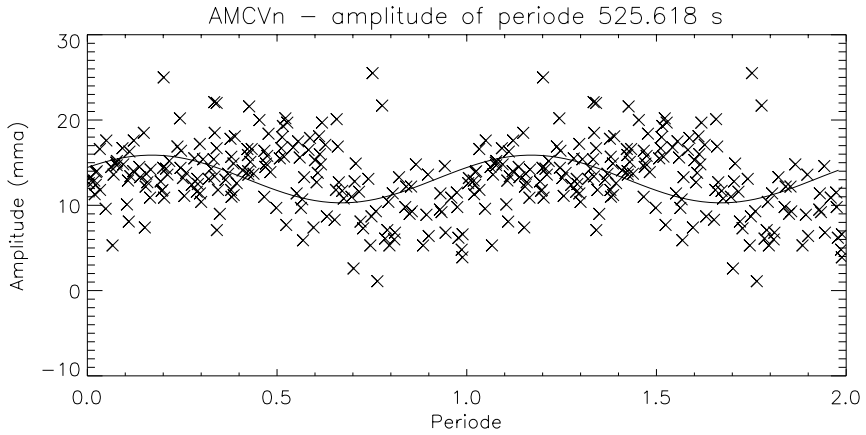

Fig. 11. The modulation amplitude of the strongest modulation h_{10} = 1902.5 μHz versus the precession period $13^{\rm h}.4$. The pulsation amplitude has been calculated by fitting the period 525.618 s to sections of the data about 4 cycles ($\sim$ 35 minutes) long. The solid line shows a linear least square fit with a period 13.32 hrs, a mean amplitude 13.1 mma and a sinusoidal variation with A = 6.1 mma

rection of AM CVn (van Teeseling 1995). The hard component is probably related to the accretion column on the white dwarf, and the blackbody source is most likely the central white dwarf or its boundary layer.

We propose that a solution to the $2\Omega_{\rm orb}$, or the "double hump" problem, is found in the noncircular shape of AM CVn's disk, combined with the m = 2, two-armed spiral. But to explain the $3\Omega_0$ we have to add a m = 3 spiral or triangular shape in the outer part, and finally a precessing, elliptical wave to completely explain the observations. Schematically the system may look as in Fig. 12.

A disk with two-fold azimuthal structure, or tidal bulges is equivalent to the Earth with lunar tides. The Earth tides are, on average, very well synchronized with the lunar orbit – but the amplitude, and to some degree the phase may vary from day to day because of local weather. Small variations in the mass transfer rate and a precessing elliptical disk may mimic local weather on earth, changing the amplitude and phase of the tidal variations on short time scales, creating differences between the predicted and observed light curve as demonstrated in Fig. 2.

The phase variability of $2\Omega_{\rm orb}$ on several short time scales (Solheim et al. 1984) may be linked to small variations in the precession rate, arising from variations in $\dot{M}_2$ or chaotic behaviour in the disk. Fig. 13 shows that the amplitude of h_{10} is modulated with the precession frequency ($\Omega_{\rm b}$). Again, we would expect the same amplitude modulation if the two frequencies are independent. A larger modulation amplitude implies a higher disk eccentricity, which occurs when the position of the secondary star coincides with the major axis of the elliptical disk, perhaps introducing increased mass transfer.

Based on this model, the disk must have a small eccentricity, which precesses with the period $P_{\rm b}$, explaining the observed superhump period of $P_{\rm s}$ = 1028.5 s. An eccentricity $e \sim 0.1$–0.2 is necessary to explain the 13.4 hr line-profile changes observed by Pattersen et al. (1993).

What can we expect for $\dot{P}_{\rm orb}$ in this model? We expect $P_{\rm orb}$ to decrease through loss of angular momentum by general relativity, which is more than compensated for by the high mass transfer which leads to orbital expansion. Assuming conservative mass transfer, $\dot{P}_{\rm orb}$ is predicted to be between 3.6 and 7.3×10^{-13} s s^{-1} (Faulkner et al. 1972). However, a wind is observed in the system, and mass and angular momentum are not conserved. Therefore we expect a somewhat larger rate of period change than predicted by Faulkner et al. Provencal et al. (1995) determined a $\dot{P}$ for the 525.6 s period of 1.7×10^{-11} s s^{-1}, a factor of 50 too large to be explained solely by GR and conservative mass transfer. Either the system is losing additional angular momentum at a high rate or the observed $\dot{P}$ is not a measure of orbital evolution.

We have now explained the modulations with the largest amplitudes in the temporal spectrum. The final question is why we do not detect $\Omega_{\rm orb}$ itself? In high inclination disks we would expect occultations due to the secondary passing in front of the disk or the bright spot, producing modulations with the orbital frequency. As shown in Fig. 12, we find that, for our choice of masses and $\Omega_{\rm orb}$, no disk occultations will take place if $i < i_{cr}$ = 61° – so disk occultations cannot occur in this case since our solution gives $i \sim 40°$.

The tidal bulges and the two spiral arms are on average stationary features seen twice per orbital period. Changes in the mass transfer rate and the disk ellipticity may change the position of the tidal bulges, which we observe as irregularities or 'phase jitter' in the light curve and the superhump period.

From UBVRI observations of the light curve, Massacand & Solheim (1995) conclude that the h_{10} modulation has equal amplitude in each band, which can be explained by the disk size and shape effects described above. This reinforces our conclusion that h_{10} is a result of changing aspects of the disk.

The h_{20} modulation has a slightly larger amplitude at longer wavelengths and may arise from the cooler, outer part of the disk (Massacand & Solheim 1995). Based on our conclusion we can now present a complete table of identification of the 4 independent frequencies in the system and their beats, harmonics, sums and differences as given in Table 4.

5.3. The 988.8 μHz modulation could be a g-mode pulsation

The 988.8 μHz modulation has many properties common with observed g-mode pulsations. It varies in amplitude on many time scales – years to even hours, perhaps explained by beating of closely spaced modes or fine structure due to rotational splitting. It has a higher amplitude in the far UV (Solheim et

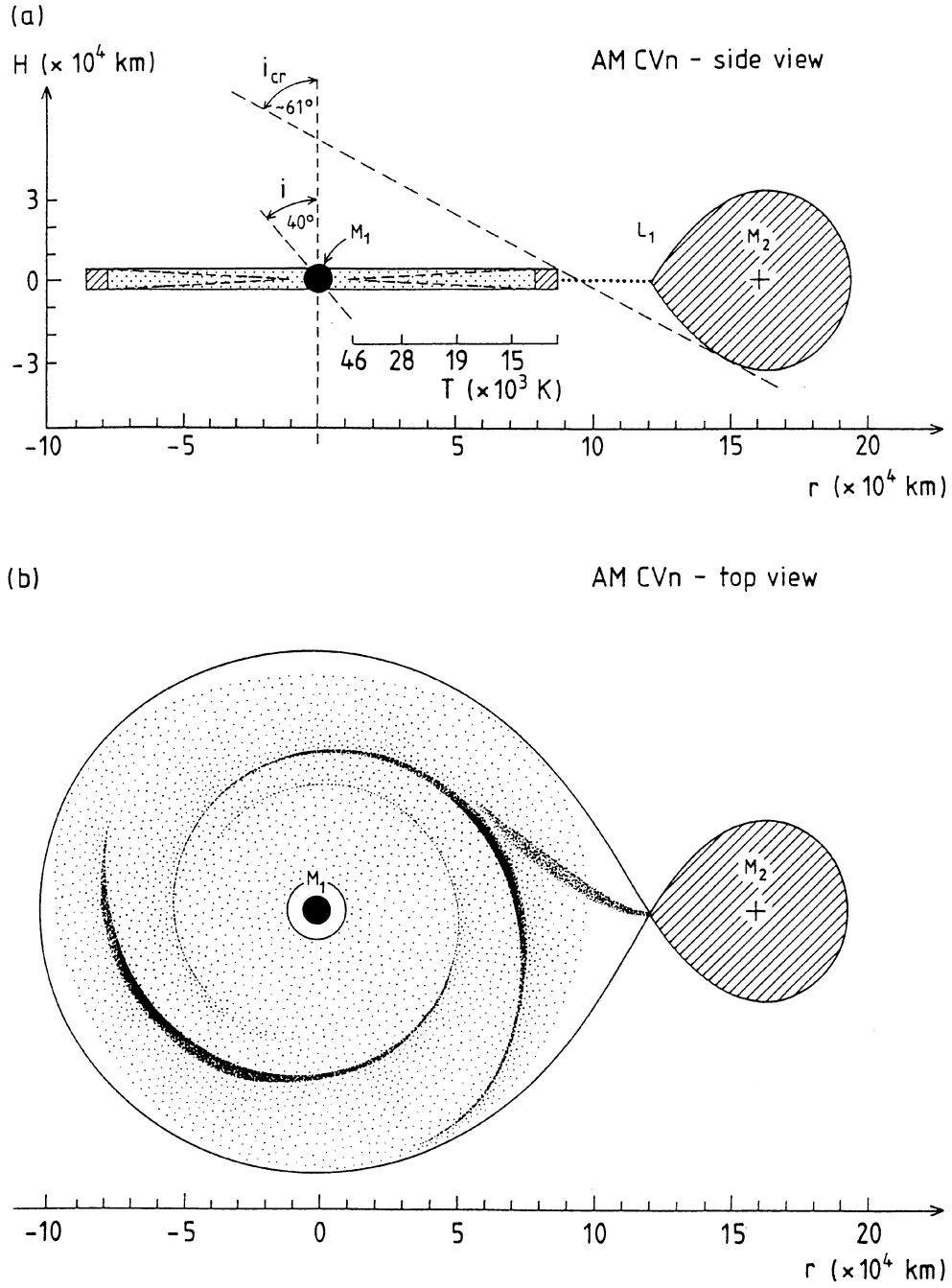

Fig. 12a and b. Geometry of a disk with strong $m = 2$ tidal response which gives rise to spiral arms, and weak $m = 3$ response which gives rise to triangular shape in the outer parts. For AM CVn the 20.8 μHz sideband indicates in addition a prograde precessing eccentricity

al. 1997). For a single white dwarf pulsator this is a result of limb darkening, which is stronger in the far UV (Robinson et al. 1995). It is also within the possible range of periods expected for DOs (Bradley 1995) and perhaps DBs with hot accreted envelopes (Nitta 1996). In order to fit the UV observation the central star of AM CVn is more likely a DO with temperature 150–180,000 K (Bard 1995; Nymark 1997).

Identification of g-mode pulsations in AM CVn opens interesting possibilities for modelling the interior of the accretor. Pulsation modes may be amplified by parametric resonance with the orbital frequency of the secondary object. This may be the first hint of a cooler star disguised with a hotter envelope, and may explain the rapid amplitude variations. Since the resonance is not exact, and the pulsation may at times be out of phase with the orbital phase, the pulsations may be damped instead of driven. Over the years the observed amplitude has changed with a factor more than ten, from 1.2 mma in 1990 to 15 mma in 1982, which is a change from 10 to 100 mma if the disk were not present (Fig. 13). When the amplitude is largest we should expect the pulses to be highly driven and non sinu-

Table 4. Explanations of frequencies in AM CVn

Frequency (μHz)	Name	Explanation
20.8	Ω_b*	Prograde ellipticity precession frequency in the disk (m = 1)
951.3	Ω_{orb}	Orbital frequency: $\Omega_{orb} = f_0$ (not observed)
972.3	Ω_s	Superhump frequency: $\Omega_s = \Omega_{orb} + \Omega_b$
988.8	?*	Probably not disk related (g-mode pulsation on the accreting star?)
1902.5	h_{10}^*	$2\Omega_{orb}$: Aspect variation of two-armed spiral (m = 2)
1923.4	h_{11}	$2\Omega_{orb} + \Omega_b$ or $\Omega_{orb} + \Omega_s$
1944.4	h_{12}	$2\Omega_s$: Pulse shape harmonic
2853.8	h_{20}^*	$3\Omega_{orb}$: Aspect variations of tidal response in the outer part of the disk (m = 3)
2874.5	h_{21}	$3\Omega_{orb} + \Omega_b$ or $2\Omega_{orb} + \Omega_s$
2895.4	h_{22}	$2\Omega_{orb} + \Omega_s + \Omega_b$
3805.2	h_{30}	$2 \cdot h_{10}$: Pulse shape harmonic
3825.9	h_{31}	$h_{10} + h_{11}$
4756.4	h_{40}	$h_{10} + h_{20}$
4777.4	h_{41}	$h_{11} + h_{20}$
5707.8	h_{50}	$2 \cdot h_{20}$ or $3 \cdot h_{10}$: Pulse shape harmonic

* These 4 frequencies are independent

soidal, generating a series of higher harmonics of the pulsation frequency. In the WET run reported in this paper, such harmonics of 988.8 μHz were not observed, due to the small amplitude (1.2 mma) of the variation itself.

The modulational frequency of 988.8 μHz found in AM CVn is near the pulsation frequencies observed for the hottest DOV stars such as RXJ 2117+34 (T = 170,000 K) (Moskalik & Vauclair 1965; Werner et al. 1996). This supports other evidence for the classification of the central star as a DO.

The disk in AM CVn stars contributes the majority of light in the optical part of the spectrum, but the contribution from the hot accretor will be relatively stronger in the far UV, predicting higher pulsation amplitudes in this spectral region. Monitoring AM CVn's light curve in the far UV over several days, would be of great importance for settling the question of g-mode pulsations in AM CVn. With such monitoring it may also be possible to detect frequency sidebands due to rotation of the white dwarf.

6. Conclusions

We set out with the hope of unlocking the mysteries of AM CVn, a helium binary with the same optical colours and temperature as observed for pulsating helium white dwarfs. The Whole Earth Telescope, which in twelve days doubled the available photometry on the object, provided a new tool to eliminate gaps in data coverage and identify periodic modulations in the system. As is the case with many past WET runs, the data reveals unexpected complexities and problems and will be a great source for future studies of the object.

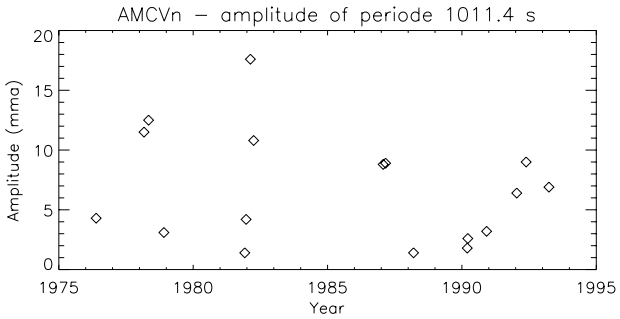

Fig. 13. The amplitude of the modulation at 988.8 μHz as observed in the period 1976–1993

AM CVn's temporal spectrum is simple, with precise integer relations between frequencies of orbital resonances, some of which with sidebands with a spacing of 20.8 μHz, which we believe are the result of superhump modulations. The stable part of the temporal spectrum can be explained by 4 independent frequencies, 2 of which we identify as the disk's response to the m = 2 and 3 terms of the tidal potential, where m = 2 is the strongest and gives a two-fold azimuthal structure as two spiral arms, m = 3 is a far weaker tidal response in the outer part of the disk, forcing it into a triangular shape. The m = 1 mode is assumed to be generated somehow, and then amplified by wave interaction as proposed in Lubow's (1991) model. This leads to a weak prograde precessing wave in the disk.

The best model which describes the data remains an ultra-short period binary undergoing mass transfer. We have improved on the original model of FFW by including a precessing elliptical accretion disk with a stationary spiral pattern, created in response to the system's small mass ratio and the close orbit. The mass transfer rate is large enough to keep the disk in a permanent superoutburst state. The temporal spectrum observed gives us means to investigate structural variations within the disk.

In addition to the stable frequencies detected and analysed, the object also displays quasi periodic modulations, which we interpret as signs of mass accretion from the disk onto the primary object. We could not identify with certainty any modulations from the central accreting star, but propose the modulation with frequency 988.8 μHz as the most likely candidate for a g-mode pulsation on the accretor, supporting the classification of the central object as a DO white dwarf. The detection of the superhump period and the orbital period, gives a mass of 1.0 $M_\odot$ for the primary object. Some parameters deduced for the system are given in Table 5.

On the observational side, we must continue monitoring AM CVn in both white light and multicolour photometry. Of particular importance is an understanding of AM CVn's photometric behaviour in the far UV, leading to determination of the temperature and hence the origin of the various modulations. To investigate the possibility of a g-mode pulsation at 988.8 μHz, a future WET campaign should be organised at a time when the amplitude of this modulation is at its highest, as was the case in

Table 5. Some parameters for AM CVn

	Parameter	Ref.
Primary mass:	M_1 = 1.0 $M_\odot$	8
Secondary mass:	M_2 = 0.09 $M_\odot$	8
Mass transfer rate:	$\dot{M}_2 = 6.4 \times 10^{16}$ g/s	2,4
Orbital period:	$P_{\rm orb}$ = 1051.2 s	8
Inclination of orbital plane:	$i \approx 40^\circ$	8
Superhump period:	$P_{\rm s}$ = 1028.5 s	8
Period change:	$\dot{P}_{\rm orb}/2 = (1.71 \pm 0.04) \times 10^{-11}$ s s^{-1}	3
Distance between primary and secondary:	a = 158 000 km	8
Radius of primary object:	r_* = 5600 km	8
Tidal radius of the accretion disk:	r_t = 15 r_*	8
Inner radius of the disk:	r_i = 2.1 r_*	8
Ellipticity of accretion disk:	$e \approx$ 0.1–0.2	1
Period of precession of elliptical axes:	$P_{\rm b}$ = 13.4 hrs	1
Structure of accretion disk	Two-fold symmetry (spirals) with three-fold perburbations in the outer parts	8
Type of primary object:	DO with hot envelope	5,8
Temperature of primary object:	$T_{\rm eff}(1) \approx$ 180 000 K	6
Type of secondary object:	Helium stellar semi-degenerate star with carbon-enriched core	7

References: 1. Patterson et al. (1993); 2. Solheim (1993b); 3. Provencal et al. (1995); 4. Bard (1996); 5. Solheim & Sion (1994); 6. Nymark (1997); 7. Savonije et al. (1987); 8. This paper

1987 and in 1995. One could then search for harmonics, multiplet splitting, and amplitude as function of wavelength for this modulation frequency.

In addition we must intensify the investigation of the other AM CVn stars. If our model is correct, they should also possess precessing elliptical disks – at least in their high state, but a superhump period may be more difficult to detect if the objects are observed at lesser inclination, which certainly is the case for V803 Cen, where we do not observe emission inside the absorption lines, as we do in AM CVn (Solheim 1993a). The most promising candidate for identification of a superhump period is EC 15330–14, which appears to have an even simpler temporal spectrum than AM CVn, and shows strong modulation at the fundamental frequency (O'Donoghue et al. 1994).

On the theoretical side, we require detailed models of helium disks atmospheres appropriate for AM CVn systems (Bard 1995). We must also produce a better model for permanent superoutbursts in helium disks (Osaki 1995; Tsugawa and Osaki 1995), and consider a detailed study of a hole in the center of the AM CVn's disk, as discussed by Provencal et al. (1995) and indicated in our analysis. In addition, we know that, whatever the surface temperature, the central white dwarfs' internal temperature profile must differ from a normal single white dwarf. We challenge theoreticians to investigate the possibility that some of the observed periods (as 1011.4 s) arise from g-mode pulsations in the mass gaining white dwarf.

We cannot continue to ignore the secondary object. Evolutionary calculations of ultrashort period binary systems undergoing mass transfer, shows that the secondary is burning helium in its core until the approach of a minimum orbital period of 10.6 minutes (Savonije et al. 1986). If the binary period is now increasing, it must have passed the minimum period. The secondary is extremely underluminous, but is blasted with radiation (Nymark 1997). Since it is still transferring helium, it must have a helium atmosphere on top of a carbon–oxygen enriched core.

Finally, we reflect upon the future of AM CVn and related systems. Although we know of only 6 such objects, there appears to be a relationship between behaviour and photometric or orbital period, and hence mass transfer rate. AM CVn's general characteristics should remain unchanged until the orbital period increases above $P_{\rm crit} \sim$ 1350 s (Eq. (3)) when disk instabilities begin to occur. AM CVn will reach this threshold in about 200 000 years, if we accept the rate of period change determined by Provencal et al. (1995) as the time scale for orbital evolution.

As it evolves, AM CVn will then look similar to V803 Cen and CR Boo, exhibiting large changes in mean magnitude. The semi-degenerate secondary will not inhibit mass transfer, and in 50–100 Myr most of its mass should be transferred. The final product may look like a single helium white dwarf with a thick, rapidly rotating atmosphere – possibly with a brown dwarf or a planet companion. The descendants of AM CVn stars should be DO or DB stars. If the mass of AM CVn is $\approx 1\ M_\odot$, and this is typical for the primary of AM CVns, then the descendants may be distinguished as DO or DB white dwarfs with higher than average masses and somewhat different pulsation pattern.

Another, less likely scenario for its evolution which needs to be explored, is that the secondary is likely to start transferring carbon-rich material to the disk when the helium envelope is lost (Savonije et al. 1986). The increased opacity of carbon compared with helium may lead to an expanding He–C mixed atmosphere – and the system may look like a R CrB object (Solheim 1996).

Acknowledgements. The first author (JES) thanks the Norwegian Research Council for travel support. He also thanks the Department of Astronomy at the University of Texas and the Department of Astronomy at the University of Cape Town for generous support during sabbatical visits. We also thank Marion Frueh who did observations at McDonald Observatory for us – and all the telescope allocation committees who allocated observing time for this project. Finally we thank the referee G. Savonije for extremely helpful comments, and to Liv Larssen for patiently working with the manuscript.

References

Bard S., 1995, University of Tromsø, Cand. scient., thesis
Bard S., 1996, in Cataclysmic Variables and Related Objects, Evans A., Wood J. (eds.), Kluwer, p. 135
Bradley P., 1995, Baltic Astronomy 4, 536
Emanuelsen P.-I., 1990, University of Tromsø, Cand. scient. thesis (in Norwegian)
Faulkner J., Flannery, B. P., Warner B., 1972, ApJ 175, L79
Hansen C. J., Kawaler S. D., 1994, in Stellar Interiors, Springer, p. 127
Heemskerk M. H. H., 1994, A&A 288, 807
Iben I., Jr., Tutukov A., 1986, ApJ 311, 742
Iben I., Jr., Tutukov A., 1991, ApJ 370, 615
Ichikawa S., Hirose M., Osaki Y., 1993, PASJ 45, 243
Kalytis R., Meištas E, Sperauskas J., 1997, Baltic Astronomy 8, in press
Kepler S. O., 1993, Baltic Astronomy 2, 515
Kruzewski, Semeniak, 1993, Acta Astron. 42, 311
Kurtz D. W., Mathews J. M., Martinez P. et al., 1989, MNRAS 240, 881
Lubow S. L., 1991, ApJ 381, 259 and 268
Massacand C. M., Solheim J.-E., 1995, Baltic Astronomy 4, 378
Moskalik P., Vauclair G., 1995, Baltic Astronomy 4, 360
Nather R. E., 1985, in Interacting Binaries, Eggleton P. P., Pringle J. (eds.), NATO ANSI, series C, Vol. 150, Reidel, p. 349
Nather R. E., Robinson E. L., Stover, R. J., 1981, ApJ 244, 269
Nather R. E., Winget D. E., Clemens J. C., Hansen C. J., Hine B. P., 1990, ApJ 361, 309
Nitta A., 1996, University of Texas at Austin, Department of Astronomy, M.A. thesis
Nymark T. K., 1997, in White Dwarfs, Isern J., Hernanz M., Garcia–Berro E. (eds.), Kluwer, p. 343
O'Donoghue D., Kilkenny D., Chen A., et al., 1994, MNRAS 271, 901
Osaki Y., 1989, PASJ 41, 1005
Osaki Y., 1995, PASJ 47, L11
Osaki Y., 1996, PASP 108, 39
Patterson J., Nather R. E., Robinson E. L., Handler F., 1979, ApJ 232, 819
Patterson J., Sterner E., Halpern J. P, Raymond J. C., 1992, ApJ 384, 234, called PSHR
Patterson J., Halpern J., Shambrook A., 1993, ApJ 419, 803
Provencal L., 1994, University of Texas, Doctoral thesis
Provencal J. L., Winget D. E., Nather R. E., et al., 1995, ApJ 445, 927
Robinson E. L., Mailloux T. M., Zhang E., et al., 1995, ApJ 438, 908
Savonije G. J., de Kool M., van den Heuvel E. P. J., 1986, A&A 155, 51
Savonije G. J., Papaloizou J. C. B., Lin D. N. C., 1994, MNRAS 268, 13
Seetha S., Ashoka B. N., Marar T. M. K., et al., 1990, in North American Workshop on Cataclysmic Variables and Low-Mass X-Ray Binaries, p. 139
Skillman D. R., Patterson J., 1993, ApJ 417, 298
Smak J., 1967, Acta Astron. 17, 255
Smak J., 1983, Acta Astron. 33, 333
Solheim J.-E., 1993a, in White Dwarfs: Advances in Observations and Theory, M. Barstow (ed.), Kluwer, p. 395
Solheim J.-E., 1993b, Baltic Astronomy 2, 445
Solheim J.-E., 1993c, in White Dwarfs: Advances in Observations and Theory, M. Barstow (ed.), Kluwer, p. 387
Solheim J.-E., 1995, Baltic Astronomy 4, 363
Solheim J.-E., 1996, in Hydrogen-Deficient Stars, Jeffrey S., Heber U. (eds.), ASP Conference Series, Vol. 96, p. 309
Solheim J.-E., Kjeldseth–Moe O., 1987, Ap&SS 131, 785
Solheim J.-E., Sion E., 1994 A&A 287, 503
Solheim J.-E., Provencal J. L., Sion E., 1997, in White Dwarfs, Isern J., Hernanz M., Garcia–Berro E. (eds), Kluwer, p. 337
Solheim J.-E., Robinson E. L., Nather R. E., Kepler S. O., 1984, A&A 135, 1, called SRNK
Solheim J.-E., Emanuelsen P.-I., Vauclair G., et al., 1991, in White Dwarfs, Vauclair G., Sion R. E. (eds.), NATO ANSI series, Vol. 336, Kluwer, p. 431
Steeghs D., Harlaftis E. T., Horne K., 1997, MNRAS 290, L28
Tsugawa M., Osaki Y., 1995, in Basic Physics of Accretion Disks, S. Kato et al. (eds.), Gordon and Breach, 1995, to be published.
Ulla A., 1995, A&A 301, 469
van Teeseling A., 1995, private communication
Warner B., 1995a, Ap&SS 225, 249
Warner B., 1995b, Cataclysmic Variable Stars, Cambridge University Press, p. 132
Warner B., Robinson E. R., 1972, MNRAS 159, 315
Werner K., Dreissler S., Heber U., et al., 1996, in Hydrogen-Deficient Stars, ASP Conference Series, Vol. 96, p. 267
Whitehurst R., 1988, MNRAS 232, 35
Winget D. E., Nather R. E., Clemens J. C., et al., 1991, ApJ 378, 326

This article was processed by the author using Springer-Verlag LaTeX A&A style file *L-AA* version 3.